



In Silico Track to Reveal a Translational Potential of Porphyrin-C60 Nanoparticles in the Ischemic Stroke Related Preclinical Studies

Valentin Fursov^{1,2,3}, Daria Zinchenko², Dmitriy Kuznetsov^{1,4*}

Abstract

The *In Silico* study on neuropharmacokinetics of some novel porphyrin-fullerene based $^{25}\text{Mg}^{2+}$ - nanocarriers was performed with an aim to optimize the preclinical research path required for both prevention and correction of brain ischemic stroke related metabolic disorders such as ATP deplete and its direct consequences. Thus, the local brain tissue hypoxia scenario is in a focus of this novel analytical approach suitable for prediction of some parameters of the ^{25}Mg – magnetic isotope effect promoted antihypoxic activities as long as they relate upon delivery, distribution and intralization of the low toxic/amphiphilic Mg^{2+} – releasing nanoparticles of PMC16 type. This is the first report ever on mathematical model applied to predict and to prove a mere phenomenon of the “cellular pump” keeping the constant traffic of PMC16 particles towards a brain hypoxia area even when/if lowest concentration of pharmacophore were the case.

Two versions of mathematical model were proposed in a present study: (a) a basic two-compartment model to describe a mechanism of the nanopharmacophore targeted delivery towards the brain ischemia area, and (b) an advanced five-compartment model, verified and supported by some specific experimental data on PMC16 distribution (CZE) in organs/tissues.

A novel procedure of the capillary zone electrophoresis (CZE) suitable for a reliable validation of the *In Silico* – predicted PMC16 pharmacophore pharmacokinetic patterns, has been proposed and discussed

For experimental verifications of the *In Silico* platform proposed, a combination of (a) the rat brain occlusion – promoted ischemic stroke model and (b) the capillary zone electrophoretic (CZE) quantification of PMC16-RX nanoparticles in cytosol fractions isolated from intact / penumbra / stroke brain areas, has been employed.

From a practical point of view, a novel *In Silico* systematic directory proposed might indicate a perspective for clear and essentially simplified plan making required to design an optimized protocol suitable for the $[^{25}\text{Mg}^{2+}]\text{PMC16}$ – related preclinical research program.

Keywords: *In Silico* models; Ischemic stroke; Pharmacokinetics; ^{25}Mg -magnetic isotope effects; Medicinal nanocationites.

Introduction

Development of a pharmacologically suitable, i.e. safe and effective, nanocarrier of Mg^{2+} ions was caused by the recent discovery of biophysical control of energy production in mitochondria through the so-called magnetic isotope effect of magnesium-25. It has been proven that only the magnetic isotope of magnesium $^{25}\text{Mg}^{2+}$ is a specific hyperactivator of most Mg^{2+} + dependent reactions of ATP synthesis in the cell. It is noteworthy that the hyperactivation of energy metabolism by $^{25}\text{Mg}^{2+}$ ions requires an insignificant amount of these ions and takes place even in the absence of oxygen (deep tissue hypoxia). Thus, the desired application of the described physical/biophysical phenomenon would be to correct the reduction of ATP production in tissues during hypoxia of any nature. To meet these expectations, a new pharmaceutical preparation based on a porphyrin-containing fullerene “ball” C_{60} (porphyrin-MC16 or PMC16) has been proposed [1,2].

Affiliation:

¹N.I. Pirogov Russian National Research Medical University, www.rsmu.ru, Moscow, Russia

²Mendeleev University of Chemical Technology of Russia, www.muctr.ru, Moscow, Russia

³Peoples' Friendship University of Russia, www.rudn.ru, Moscow, Russia

⁴N.N. Semenov Federal Research Center for Chemical Physics, Russian Academy of Sciences, www.chph.ras.ru, Moscow, Russia

*Corresponding author:

Prof. Dr. D.A. Kuznetsov, N.I. Pirogov Russian National Research Medical University, www.rsmu.ru, Moscow, Russia.

Citation: Valentin Fursov, Daria Zinchenko, Dmitriy Kuznetsov. *In Silico* Track to Reveal a Translational Potential of Porphyrin-C60 Nanoparticles in the Ischemic Stroke Related Preclinical Studies. Journal of Psychiatry and Psychiatric Disorders. 9 (2025): 314-330.

Received: October 17, 2025

Accepted: November 24, 2025

Published: December 15, 2025

Both the substrate and oxidative phosphorylation pathways are Mg^{2+} dependent processes and, therefore, can be accelerated up to 2.5 times by ultramicro amounts of $^{25}Mg^{2+}$, the only magnetic isotope of magnesium, in contrast to the nonmagnetic isotopes $^{24}Mg^{2+}$ and $^{26}Mg^{2+}$ [3]. Simple “endosmotic pressure” causes the replacement of one Mg isotope by another (all of them are stable) in the active site of the creatine kinase (CK) [4].

This contributes to the manifestation of the magnetic isotope effect of $^{25}Mg^{2+}$, which, as shown to date, is an important hyperactivating element of magnesium-dependent control of ATP synthesis [3-6]. This makes the targeted delivery of the aforementioned magnetic isotope (nuclear spin $+5/2$, magnetic moment 0.85 of Bohr magneton, proportion in the natural mixture of isotopes 11%) to cells / tissues affected by hypoxia a really important pharmacological task. Nanoparticles capable of exchanging Mg^{2+} ions may be a suitable means of such delivery. For this purpose, low toxicity ($LD_{50} = 896$ mg/kg, rats, i/v), amphiphilic (water solubility 430 mg / ml, pH 7.40), capable of clustering, membranotropic particles with a size of 1.8 nm based on fullerene C_{60} [1,2]. This new drug, which has noticeable cationic properties (Figure 1), is a monoadduct of iron-containing porphyrin with the classic buckminsterfullerene - buckminsterfullerene (C_{60})-2-(butadiene-1-yl)-tetra-(o- γ -aminobutyryl-o-phthalyl)-ferroporphyrin. Based on the synthesis methodology, it was named “Porfillerene-MC16” or PMC16 for short (Figure 1).

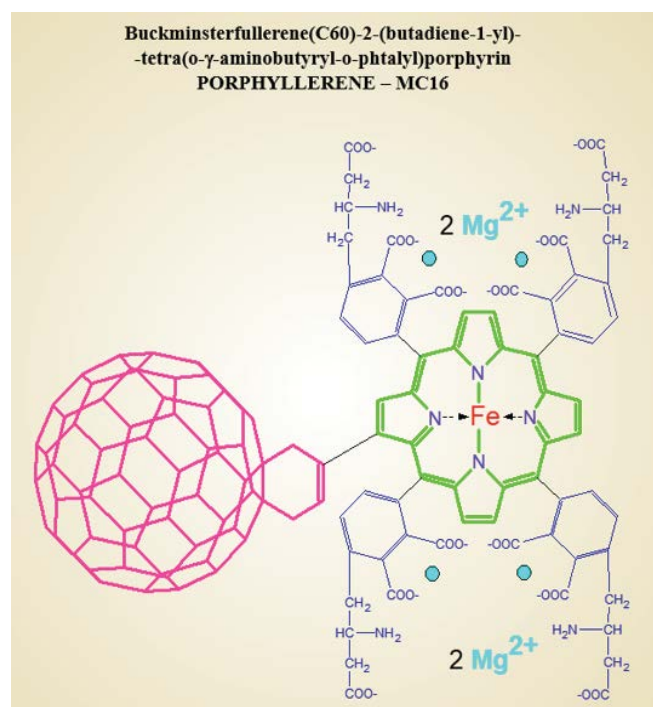


Figure 1: Monoadduct of iron-containing porphyrin with classical buckminsterfullerene - buckminsterfullerene (C_{60})-2-(butadiene-1-yl)-tetra-(o- γ -aminobutyryl-o-phthalyl)-ferroporphyrin (“Porfillerene-MC16” or PMC16) [1,2].

You can expect this drug to fulfill at least two desires. First, its unique structure could allow the drug to serve as a nanocation exchanger both in vitro and in vivo as a result of “smart release” of magnesium in case of hypoxia-induced acidosis. Secondly, the porphyrin domain of PMC16 may provide tissue selectivity in relation to interaction with cell-specific porphyrin receptors located on the mitochondrial membrane of myocardiocytes, where this has already been proven [7-9], but also on the membranes of other cell types, and in particular, cells of the brain that have undergone oxygen starvation. This will allow for a truly targeted delivery of drugs to the area of hypoxia in the case of ischemic stroke. Considering the particle size of PMC16 (1.8 nm), drug penetration into mitochondria looks realistic [1, 2]. The pharmacokinetics of PMC16 and the recognition of the drug by the receptor can facilitate or prevent this.

Noteworthy, the cation – exchanging nanoparticles (PMC16 family members) we’re taking here for granted as the “safe-n-stable” adducts of fullerene – C_{60} are all known water soluble products with the marked antioxidant, i.e. potentially antihypoxia, properties for themselves – even once applied unloaded by any metal ions [10-13]. Thus, amphiphilic fullerene – containing compounds are, most likely, capable to emphasize the magnetic isotope effects of $^{25}Mg^{2+}$ on ATP-synthase and nucleotidyl kinases reaching both ATP hyperproduction and an oxygen consumption decrease [11, 12] so beneficial for neuroprotection in the hypoxia – damaged brain tissue regions. The main directions in the modern pharmacology of fullerenes are associated with the problem of targeted drug delivery, since the possibility of these membranotropic nanoagents has already been shown to serve as specific carriers for organic / bioorganic drugs [14, 15].

However, as far as we know, with the exception of [1, 2], no in vitro and in vivo studies of the cation exchange activity of fullerene C_{60} derivatives have been carried out. In view of this, based on the already known data describing the experimental pharmacokinetics of PMC16 for the mitochondria of myocardial cells, it is possible to simulate *In Silico* the processes of targeted drug delivery, which is very promising for optimizing the program of preclinical studies of the drug, incl. for other nosologies.

At the same time, it should be noted that, in the absence of any studies known to us on modeling the pharmacokinetics of targeted delivery of nanopreparations based on fullerene-porphyrin adducts, the creation of *In Silico* models of the pharmacokinetics of targeting and selective accumulation of PMC16 nanoparticles is extremely important for optimizing further research in this area and possesses all the necessary novelty and relevance. Talking about the direct and obvious practical benefits that are expected to be obtained through the proper use of mathematical modeling in determining the plan for preclinical studies of antihypoxic drugs, which in itself,

undoubtedly, should be noted, such modeling is an essential requirement for optimizing the research plan for all new drugs. In particular, the applied pharmacological potential of such an approach based on the *In Silico* computational experiment can be perceived as an "encouraging breakthrough" for creating a new element in the strategy of preclinical studies for the prevention and / or correction of metabolic disorders of cerebral ischemia, based on the introduction of paramagnetic isotopes of bivalent metals, released and delivered by amphiphilic nanocation exchangers belonging to the superfamily of PMC16 (C_{60} -porphyrin) nanoparticles [16].

There is also one specific point we should not forget talking of an applied validity of *In Silico* research in molecular pharmacology/toxicology as a whole: a variable and contraversal bioethical problems could be better resolved while the *In Silico* studies would allow to avoid some certain experimental efforts in a course of in vivo segments of preclinical trials [17]. This should be also correct for the early steps of the new pharmaceutical's clinical trials and related research. The so-called "sovereign trend" in the computational modeling of pharmacological processes within the framework of the modern preclinical research paradigm has already had a significant impact on the development of drugs in experimental neurology and neuropharmacology [18-20]. This correlates with the PubMed statistics showing a noticeable increase in the number of publications on the above issue [21]. This work is part of a broader study devoted to the development of a new nanopharmacological approach to the prevention and treatment of local hypoxia syndrome of ischemic cerebral stroke by targeted delivery of $^{25}Mg^{2+}$ cations to the area of cerebral infarction through targeted delivery of porphyrin-fullerene nanoparticles as membranotropic carriers that release $^{25}Mg^{2+}$.

Results and Discussion

In experiments on laboratory animals for the case of myocardial infarction, certain significant characteristic features of the pharmacokinetics of PMC16 were found, which make it unique and super promising in comparison with conventional drugs, not belonging to the nano-group drugs. One of these proven experimentally remarkable features of PMC16 nanoparticles is their long-term retention in tissue and especially inside the mitochondrial membranes of myocardiocytes, the reasons for which have not been studied, but the most likely explanation for this phenomenon may be the presence of protein receptors in these membranes with high affinity for PMC16, i.e. in the presence of signaling proteins in the cell membranes, which are responsible for the selective recognition of the drug. Simple signaling proteins of this type are known for a number of porphyrin metabolites [22-26].

Another important experimentally [27-31] discovered feature is that the accumulation of particles in the ischemic zone occurs even at low concentrations of PMC16 in the blood. As for the methods of targeted delivery themselves, to date, in relation to this very peculiar group of nanodrugs, exclusively magnetic and immunological methods have been studied [22-24]. As far as we know, with the exception of works [1, 2], no studies of the cation-exchange activity of fullerene C_{60} derivatives have been carried out. On the other hand, this is exactly the activity that is required for the delivery of $^{25}Mg^{2+}$ cations to hypoxic cells and tissues. According to our point of view, the aforementioned targeted delivery can help compensate for hypoxia-induced ATP loss due to the known ^{25}Mg -dependent hyperactivation of both oxidative and substrate ADP phosphorylation pathways during ATP synthesis in the cell [3-6]. As can be seen from the data presented in [1, 2], due to its cationic properties, PMC16 has the necessary potential as a carrier of Mg^{2+} ions. It is noteworthy that this drug can act as "smart nanoparticles" capable of releasing magnesium in response to an increase in the acidity of the medium [1, 2]. At the same time, it was found that PMC16 clustering is also pH dependent. These facts look attractive in light of the data on the molecular pathogenesis of hypoxia, according to which tissue acidosis is a direct natural metabolic consequence of hypoxia of any kind [2, 6]. Thus, when $[^{25}Mg]$ PMC16 is administered in vivo, acidosis-induced $^{25}Mg^{2+}$ release can be expected. The amphiphilic nature of this drug [1, 2] also supports these expectations, since the dual solubility of a drug usually correlates with its membranotropic properties [9, 22].

In addition, the absence of allergenic properties and inflammatory effects found in most of the ever studied fullerene derivatives [29, 30] and, as a rule, a high degree of "biocompatibility" [31] allow experimental studies of the safety and pharmacological activity of PMC16 *in vivo*.

All these specific features of PMC16, despite the extremely poor knowledge of the underlying mechanisms, must be taken into account when creating mathematical models underlying *In Silico*, using a system of equations demonstrating similar dynamics. And further, such equations, using well-known mathematical tools, can be brought to a fairly good agreement with the available experimental data. This is the main idea of the fundamental solution of the *In Silico* problem of a "magic bullet" for the targeted delivery of nanopreparations of the PMC16 type to the problem area under the conditions of the complexity of so little knowledge of the physicochemical mechanisms of the entire set of processes in the body.

We are talking about the targeted delivery of the drug to the hypoxia zone: whether it is the myocardial region, the focus of ischemic stroke in the brain, or any other area of the body or organ where cells lack oxygen, including its complete absence.

The *In Silico* pharmacokinetics of targeted delivery of PMC16 is based on the idea of using the peculiarity of the course of the pathologies under study, which, as is known, the body responds to the development of the inflammatory process to the pathologies that accompany heart attacks. And for the vessels penetrating such zones of inflammation, an increased distance between epithelial cells is characteristic, which is not observed outside the zone of inflammation. So the body locally reacts to the problem and increases the throughput of the vascular sections in the hypoxic zone in order to provide an increased flow of substances from the blood that are necessary to eliminate the problem situation. Thus, PMC16 nanoparticles, even when assembled into clusters, will selectively penetrate into the inflammation zone, where they will be captured by the cell membrane, even in the absence of any driving force, except for those arising from Brownian motion. When a nanopreparation is injected directly into the circulatory system, a single-compartment model of pharmacokinetics is quite sufficient. The two-compartment model and multi-compartment models at this stage will only make the initial system of differential equations heavier, and it makes sense to resort to them at the stage of *In Silico* detailing if you need to describe in more detail other subtle processes or change the method of drug administration. Nevertheless, for convenience of understanding, we represent our system in the form of two chambers separated by an impenetrable partition, which is a surface of area S with a local porosity in some area with a total area s as shown in Figure 2.

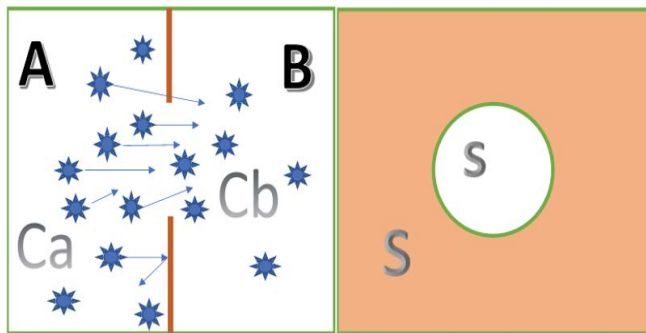


Figure 2: The graphic model of the system in the form of two chambers A and B separated by an impenetrable partition, which is a surface of area S with a local porosity in some area with a total area s . C_A and C_B are the concentrations of nanoparticles in the chambers.

The two areas that are separated by a septum are the circulatory system and the extracellular space. Let us designate these chambers by the letters A and B. Simultaneous administration of the drug at a concentration of C into the circulatory system at the time $t_0 = 0$ will increase its concentration in the blood (chamber A) from 0 to $C_A(0) = C$, while at this moment in the intercellular space (chamber B) the concentration of the drug will be $C_B(0) = 0$. Assuming in our case the system is closed, according to the second law of thermodynamics, it will tend to equilibrium, leveling the

concentrations between the chambers, and a substance flow proportional to the ratio of the pore areas and the partition area s/S will pass through the surface S . The driving force behind this process is the concentration gradient. Then the flow of matter passing from chamber A to chamber B according to Fick's 1st law can be written in algebraic form by the formula:

$$W = -\frac{s}{S} D * \text{grad} C, \quad (1)$$

where W is the substance flux (PMC16 nanoparticles), s/S is the ratio of the area of the vascular system in the area of inflammation to the total area of the circulatory system of the body, D is the diffusion coefficient, $\text{grad} C$ is the concentration gradient. For three-dimensional space

$$\text{grad} C = \nabla C(x,y,z) \quad (2)$$

In our case, for a point (global) model, the spatial coordinate is not essential and is not used, and formula (1) can be rewritten as:

$$W = -\frac{s}{S} D \Delta C = -\frac{s}{S} D * (C_A - C_B), \quad (3)$$

where C_A is the concentration of nanoparticles in the blood, C_B is the concentration of nanoparticles in the intercellular space of the inflammation zone.

The balance equation for any moment of time $t \in [0, t]$, can be written as follows:

$$C = C_A + C_B \quad (4)$$

In this case, it follows from Eq. (3) that at a certain point in time, the concentrations in both chambers become equal and the flow of nanoparticles from the blood into the intercellular space will stop. However, in practice this does not happen, since it was already noted above that the transfer of PMC16 to the ischemic zone continues even at extremely low concentrations of the drug in the blood. This can only be the case if the substance is continuously removed from zone B. The gradient will then remain positive as long as there is substance in Chamber A, down to the lowest concentrations. In this case, the system becomes open, and the balance equation (4) is not observed in it. The reason for this behavior of the system is the membranotropy of PMC16, which, being actively absorbed by cells, is excreted from the intercellular space at a certain rate e . Then the change in C_B concentration in chamber B can be written in differential form as follows:

$$dC_B/dt = -eC_B \quad (5)$$

It should be borne in mind that in chamber A the concentration of C_A also decreases with some total rate v due to various reasons: self-decay, phagocytosis, absorption by other cells, natural elimination, etc., which can be written down:

$$dC_A/dt = -vC_A \quad (6)$$

Then the basic system of ordinary differential equations of the point mathematical model can be written in the form:

$$\begin{aligned}\frac{dC_A}{dt} &= -\frac{s}{S}D(C_A - C_B) - vC_A \\ dC_B/dt &= \frac{s}{S}D(C_A - C_B) - eC_B\end{aligned}\quad (7)$$

Taking into account that the rate of elimination from the intercellular space in the area of inflammation e due to the capture of PMC16 nanoparticles by the mitochondria of cells is much higher than the rate of elimination of nanoparticles from the circulatory system v , in a first approximation it can be neglected. Then system (7) can be rewritten as:

$$dC_A/dt = -\frac{s}{S}D(C_A - C_B) \quad (8)$$

$dC_B/dt = C_B - eC_B$ By specifying the initial conditions at $t_0 = 0$, $C_A(t_0) = C$ is the initial dose of the preparation, $C_B(t_0) = 0$, can solve the Cauchy problem for the system of ordinary differential equations (8).

The resulting system of equations was simulated in MATLAB / SIMULINK version 2021b and studied for different model values of the parameters s , D , e . The curves of the calculated dependences $C_A(t)$, $C_B(t)$ are shown in a series of Figure 3.

In this paper the investigation of non-equilibrium systems within the synergetic approach is applied, which is known as the 'parametric analysis'.

In Figure 3 shows a general view of the pharmacokinetic curves of PMC16 concentrations in the circulatory system (C_A) – black line and intercellular space of the inflammation focus (C_B) – red line with a single intravenous / intra-arterial injection of the drug, calculated *In Silico* for arbitrary values of the parameters s , D , e at the time interval t : $[0, T]$, $T = 20$ hours, $T_{1/2} = 9,0$ hours.

The goal of Figure 3: we demonstrate the general view of pharmacokinetic curves the model gives. This view corresponds to their classical shape. As can be seen from the figure, the graph of the calculated graph of pharmacokinetic dependences quite adequately corresponds to the general form of pharmacokinetic curves, with the only feature that the decrease in concentration in the intercellular space is more gentle (red curve C_B), in comparison with the classical curves of pharmacokinetics. This means that the drug is retained in the blood much longer (dynamics of the C_A curve) and the transport of the drug into the extracellular space does not stop until the smallest drug concentration in the bloodstream.

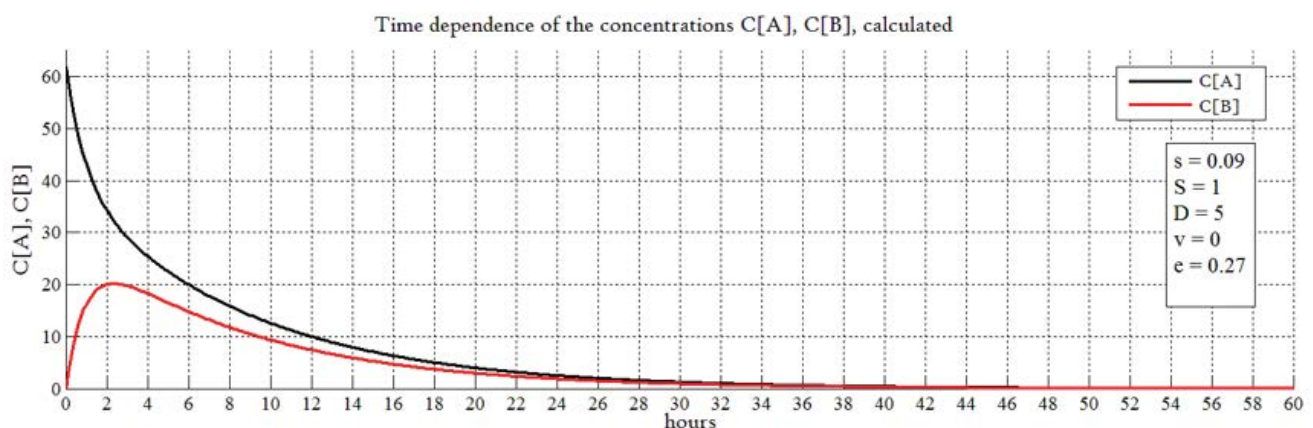


Figure 3: General view of the pharmacokinetic curves of PMC16 concentrations in the circulatory system (C_A) – black line and intercellular space of the inflammation focus (C_B) red line after a single intravenous / intraarterial injection of the drug, calculated *In Silico* for arbitrary values of the parameters s , D , e over a period of time t : $[0, T]$, $T = 20$ hours, $T_{1/2} = 9,0$ hours.

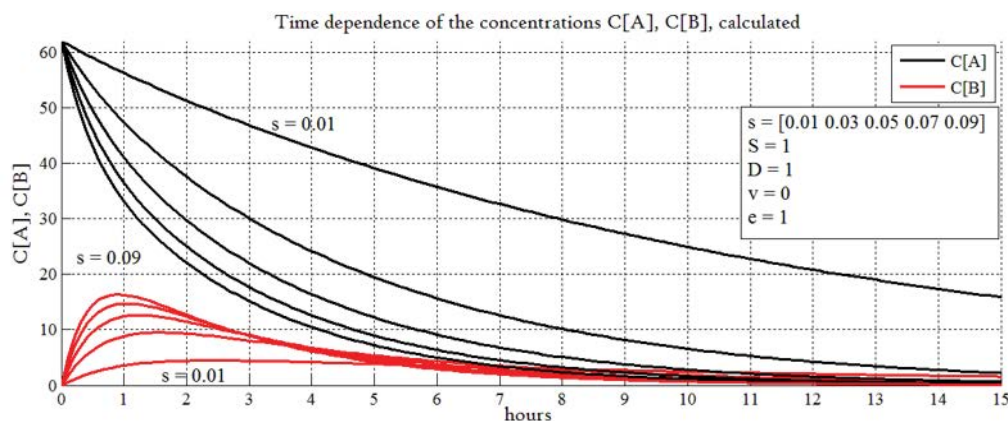


Figure 4: Behavior of pharmacokinetic curves with changing parameter s (local size of the inflammation zone during hypoxia) and fixed D and e .

In this sense, the parameter 's' plays an important role in reflecting the supply of the preparation from bloodstream to intercellular space. However, it is not definitive in describing the experimentally identified [21] specific of the targeted PMC16 delivery, including the peculiarities of its retention in ischemic cells, even in the case of low initial doses of the injected preparation. The problem is solved via the entire mathematics of the model. Prior to reaching the cells hit by ischemia, the preparation must somehow proliferate into the intercellular space. The blood vessel wall is the first barrier the PMC16 must penetrate to get into the intercellular space. The parameters' is introduced to narrowly characterize this particular phase of the pharmacokinetic process. No doubt, there exist various mechanisms of the penetration of medications into the intercellular space, and indirectly they are just as well accounted for by 's'. It is known that in the inflammation zone the organism reacts by increasing the intercellular distance between the epithelial cells of the vessels in order to provide for enhanced supply/ejection of the necessary substances and metabolic products, and this mechanism may be considered definitive for the delivery of PMC16. Thus, 's' simultaneously describes the degree of inflammation, which may be considered to be proportional to the area of the pores wide enough for the penetration of the PMC16 nanoparticles and their clusters circulating in the bloodstream into the inflammation zone. The concentration gradient (3) is the driver of this flow (or a flow of any other substance), and the PMC16 supply would have been terminated fairly fast as the concentrations balance each other, were it not for the mechanism which we call the cellular pump, thanks to which PMC16 is being intensely eliminated from the intercellular space, being actively absorbed by cell in the state of hypoxia. Therefore, the concentration gradient, and, consequently, the flow of PMC16 to the inflammation zone (in contrast to other substances) is sustained up to extremely low concentrations in the bloodstream, which corresponds to the experimental picture [21].

Preliminary data from our *in vivo* studies confirm the adequacy of the presented in this article *In Silico* model (Tables 1 and 2). A detailed report on the results of these experiments will be given in our next article, which will be devoted to improving the model presented in this article and linking *In Silico* to experimental data using transfer functions.

Thus, we can investigate both the penetration of PMC16 nanoparticles into the tissues and the distribution of their components, including the released Mg^{2+} . Parameter 's' is obviously also a characteristic of the inflammation severity of ischemic strokes. However, the principal goal of this parameter is to characterize the degree of the local porosity increase of the vascular bed in the inflammation area due to the increase of the intercellular space of vascular cells and, consequently, the amount of the penetrating (into the intercellular space of the inflammation area) PMC16

nanoparticles from the blood flow. In case of no inflammation $s = 0$, meaning that PMC16 nanoparticles do not penetrate the intercellular space. With its increase the 'porosity' of the vascular bed in the inflammation area increases in proportion to the inflammation degree, which leads to the increased drug inflow from the blood stream. The exact dependence of 's' parameter value on the level of inflammation in case of an ischemic stroke has to be researched separately and is not within the scope of this study.

We might stress it out here that a particular advantage of this *In Silico* path would allow to avoid a routine post-experiment data description/treatment [8,9,11,12,21,20] due to computational prognostic power realized by an interactive taking into account of known PMC16 pharmacology, ^{25}Mg – MIE mammalian tissue hypoxia and BBB functional parameters-including the stroke related peculiarities [13, 20, 22, 24, 28].

This itself has been deliberately done to make intriguing a forthcoming comparison of our *In Silico* derived prognosis (A) with the *further experimental* data (B), whatever difference and/or similarity between (A) and (B), would be found out then. So the next anticipated step in our ongoing work is expected to be a testing quest for a key point of present study which is a prognostic validity of our *In Silico* method.

This is exactly how we could verify both scientific and applied pharmacological significance of the latter. Meanwhile, however, we're describing here a new mathematical model which is nothing but a preliminary move towards the next, experimental, phase of this current multi-stage research. After all, a specification of this *In Silico* paradigm is, of course, mandatory to establish/defend a priority for it.

The results of *In Silico* parametric analysis of the pharmacokinetic model are shown in Figures 4-6.

In Figure 4 with fixed D and e, the behavior of the pharmacokinetic curves with a changing parameter s is shown. The dependences shown in the graph reflect the behavior of the system (changes in the concentrations of PMC16 in the blood and intercellular space of the inflammation zone) depending on the local size of the inflammation focus.

In Figure 4 we study the response of the model to the inflammation level. Following parametric analysis of information systems method, we fix the values of parameters 'D' and 'e' and change only parameter 's'. Thus, we study how the inflammation degree influences the model behavior.

The parameter "S" represents the area of the vascular system of a living object and is designed to adjust to the appearance of a laboratory animal for *in vivo* research. As you know, the area of the circulatory system is different in different biological species. In this paper, we do not touch this aspect and take $S=1$ everywhere.

It can be seen from the figure (black curves C_A) that with an increase in the size of the inflammation focus, the concentration of PMC16 in the blood decreases the faster (the curve falls the steeper), the larger the size of the inflammation zone, which quite naturally and adequately reflects the behavior of the real system. In the case of a large volume of inflammation, the drug remains in the blood for much less time. In this case, in order to achieve a continuous therapeutic effect, the frequency of injections and / or the dose must be increased.

The behavior of the PMC16 concentration curves in the intercellular space of C_B (red curves) shows that the larger the size of the inflammation focus, the sharper the increase in the PMC16 concentration in the intercellular space of the focus at the time of its introduction, but also faster and more abruptly decreases. It is important to note that the maximum concentration of the drug in the intercellular space of the inflammation zone also strongly depends on its size. Analytical data presented in Figure 4 are important for the selection of individual therapy algorithms.

Figure 5 shows the behavior of the system for different 'D' and fixed 's' and 'e'. As you know, the diffusion coefficient is numerically differentiated in different organs and tissues. As can be seen from the graphs shown in the figure, when 'D' changes, the dynamics of the system also changes. Thus, by changing 'D', it is possible to tune *In Silico* selectively for hypoxia in different organs and tissues.

Here we study the impact of diffusion (parameter 'D') on the model behavior. It's important to consider the diffusion rate, because it's important to know if the model is applicable to various tissues and organs and if its prognostic and analytical properties can be enlarged. Moreover, the histology of the stroke area is inhomogeneous. This is also considered through 'D'.

The diffusion rate is different in different organs and tissues. There are methods to measure it. Diffusion is a process of the penetration of molecules and atoms of a substance between atoms and molecules of another substance, the process leading to the balancing of concentration over the volume

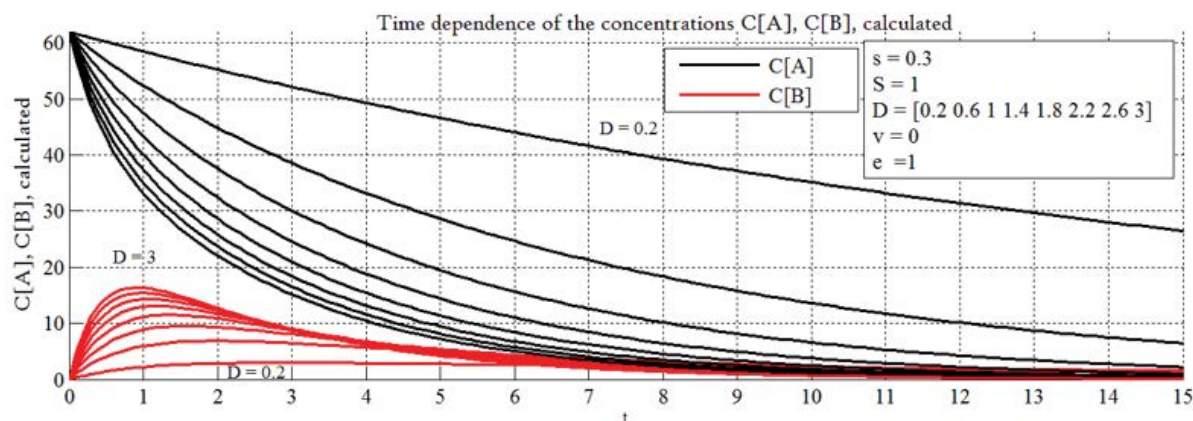


Figure 5: Changes in PMC16 concentrations in blood (black line) and intercellular space (red line) with changes in diffusion coefficient D at fixed s and e.

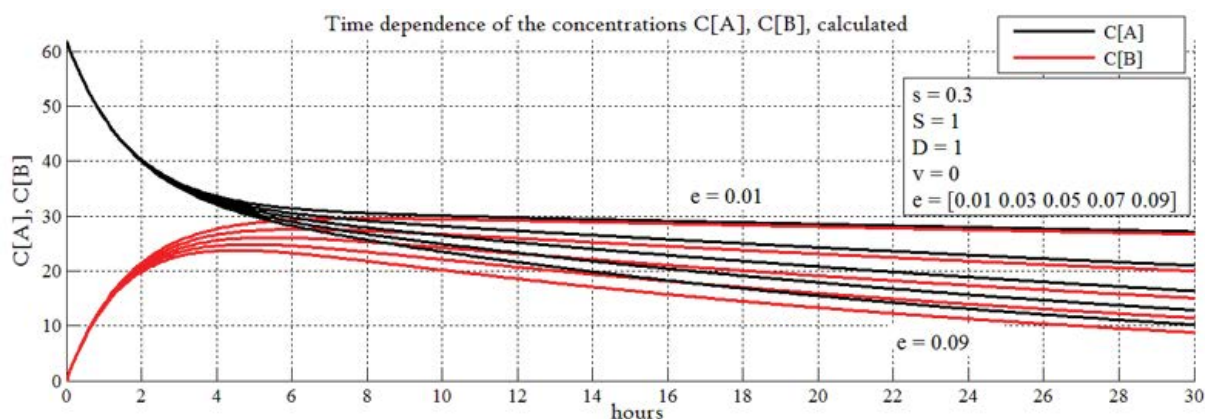


Figure 6: Changes in the concentration of PMC16 in the blood (black curve) and the intercellular space of the inflammation zone (red curve) with a change in the rate of uptake of nanoparticles by cells e of constants 's' and 'D'.

considered. The measured apparent diffusion coefficient (ADC) is a quantitative parameter of diffusion (the motion of water molecules) into tissues and is calculated using the diffusion-weighted imaging an MRI (DW-MRI) [42]. The DW-MRI are an indispensable instrument for studying the central nervous system, and apply to the identification of acute ischemic attacks as well as to the differentiation brain tumors or the diagnosing of brain infections. DW-MRI relies on the chaotic Brownian motion of water molecules in the space outside and inside of cells or inside of blood vessels. The density and size of tissue molecules, along with the presence of damaged membranes, create resistance to the motion of water molecules. This resistance may be estimated quantitatively with the help of the measured ADC. The units are mm²/c. There is no unity of opinion on the subject of the range of normal diffusion, but the respective values should depend on the specific organ and the pathology studied [43]. Some useful ADC values can be found in [44-47]. In our study, the parameter 'D' is preparation-specific to PMC16 and its numerical value does not have to match the ADC value found in literature for organs and tissues, but there may be reasonable correlation between them. Additional *in vitro* and *in vivo* studies are needed to assess the correlations exactly, for a PMC16 preparation-specific diffusion rate, as well as to obtain exact numerical values for 'D'.

It is also drug-specific. It means we speak about the diffusion of some substance in some media. In our model 'D' is a drug-specific to PMC16 and to the selected organ (in this case brain) diffusion rate. It should be taken into account that brain is histologically inhomogeneous, especially if we speak about the structure of the ischemic stroke focus. This is a separate complex issue.

In Figure 6 shows the change in the concentration of PMC16 in the blood (black curve) and the intercellular space of the inflammation zone (red curve) with a change in the rate of uptake of nanoparticles by cells *e* of constants 's' and 'D'.

Here we study the impact of parameter 'e' characterizing the absorption rate of PMC16 nanodrug by a cell. Measuring parameter 'e' at fixed 'S' and 'D', we study pharmacokinetic properties of the model. The biophysical and biochemical properties of the process are complex, not yet fully investigated and are specific for the drug. We don't consider parameter 'e' a constant. PMC16 has a high level of membrane tropism. The rate of its absorption by cells will probably depend on the degree of ischemia and the need of the cell in ATP, which the cell compensates due to the released PMC16 ²⁵Mg²⁺ nanoparticles.

The behavior of the curves confirms the experimentally found above-described unique properties of PMC16 to selectively enter the hypoxia zone even at the lowest blood concentrations. It can be seen from the graphs that the selective flow of nanoparticles into the intercellular space of

the inflammation zone continues to the lowest concentrations of nanoparticles in the blood. As you can see, the lower the concentration in the blood, the more the black and red curves are attracted to each other as the concentration decreases. Moreover, the lower their concentration in the bloodstream decreases, the higher the specific proportion of particles drawn into the intercellular space of the hypoxia focus. Moreover, for a certain *e*, the model shows "sticking of curves" (top pair of graphs), corresponding to optimal therapeutic conditions, when the entire drug is absorbed by cells with the greatest efficiency. Here we also observe the longest retention of nanoparticles both in the circulatory system and in the intercellular space of the hypoxia focus.

The parameters 'D' and 'e' are introduced to tune *In Silico* to the organ, for which hypoxia is being simulated, and to the corresponding rate of the absorption of the preparation. Thereby, the universality of the model is ensured as well as its applicability to various locations of the hypoxia such as the brain, the heart muscle, etc.

As noted earlier, parameter *e* characterizes the rate of drug uptake by PMC16 cells. And this process gives, in addition to diffusion, an additional driving force for the directed transfer of PMC16 nanoparticles to the hypoxic zone. Such a process can be compared to a pump that is additionally turned on, enhancing the transfer of matter. But it should be noted that this transfer is enhanced selectively, and not for any substance circulating in the blood, but only for PMC16 nanoparticles. It can be assumed as an explanation for the described phenomenon that the rate of absorption of PMC16 by cells depends on the degree of their need for oxygen for the production of ATP, which is a magnesium-dependent process, lacking which the cells strive to replenish it with the greater intensity, the more they lack oxygen. And ²⁵Mg²⁺ is the only source for the production of ATP under anaerobic conditions. Therefore, the greater the requirement of cells for ATP, the more intensively they absorb PMC16 nanoparticles, which are practically the only source of ATP production under hypoxic conditions.

A major key point of experimental verification for such an *In Silico* paradigm as ours is a prove for both BBB permeability and the brain cell intralization as regards specifically to PMC16 nanoparticles. This task has been solved as seen from Tables 1,2. Noteworthy, the brain stroke damaged tissue areas were also accessible for PMC16 (Table 2).

Thus, a relatively low "mass amount level" of the NP intralization in rat brain cells (Table 1) might have nothing to do with the agent's anticipated pharmacological impact since the latter would be determined by extraordinary ATP overproduction anyway, i.e. by the direct and inevitable result of ²⁵Mg²⁺- MIE phenomenon. Needless to outline that the drug intralization itself is a true priority in advanced pharmacokinetics studies.

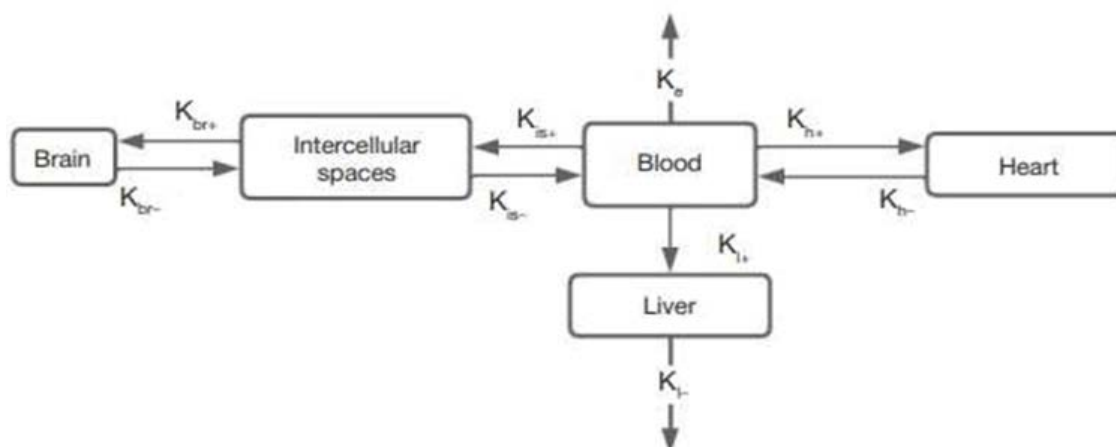


Figure 7: A scheme of the five-compartment model of PMC16 pharmacokinetics

A simple one-step ultracentrifugation of the mammalian tissue homogenates, usually pre-treated with Triton X-100, 105,000 g – 150,000 g (*Methods*), are to provide a reliable separation of cytosol from the cell organella as well as from ribosomes, ribosome subunits, and membrane debris. Being a total cytoplasm compounds solution, the S125 fraction, therefore, is a perfect material to use in drug – cell intralization research [3,4,10].

Although the results presented looks quite selfsufficient, it should be nonetheless stated that the resolution and sensitivity of our CZE procedure are good enough to find out low but detectable level of PMC16-RX rat brain uptake estimated as 4.0 – 8.0 ng per 1.0 mg of total S125 protein. This amount of NP is detectable 12 hrs after a single i.v. injection of the agent. A CZE/PMC16-RX calibration data beyond (Table 1). So, the blood – brain barrier penetration for xenobiotic tested has been clearly shown (Tables 1,2).

Five-compartment (advanced) model

Our Five-compartment (advanced) model is based on the common assumption that a nanoagent spreads throughout the body with the bloodstream, entering the heart, the liver, and the brain, and is cleared naturally afterwards. At the same time, the post-ischemic inflammation area of the brain accumulates the nanoagent faster, which is explained by increased permeability of vascular walls in this area due to the loosening of intercellular adhesions in the endothelium. The model is represented by ODE system (9) and illustrated in Figure 7.

According to this Scheme, a single i.v.injection of PMC16 NP leads to a fast formation of their initial blood plasma content. Further, the circulation directed distribution of nanodrug provides a retention of it in certain organs, such as the brain, heart and liver which has been experimentally proven earlier [12, 14, 21, 40, 55]. Noteworthy, a part of these PMC16 NP becomes a subjects for assimilation of the cells, while the rest of them moves back to blood circulations

system. That means, starting with the very moment of injection, a certain concentrations of drug – in every time point since then – are to get reached in these particular organs (C_b , C_l , C_h , C_{is} and C_{br}), which were computationally estimated within a paradigm of our model.

Here: C_b – concentration of nanoparticles in blood plasma, C_l – concentration of nanoparticles in liver tissue, C_h – concentration of nanoparticles in myocardium, C_{is} – concentration of nanoparticles in intercellular space of the brain tissue, and C_{br} – concentration of nanoparticles inside the brain cells.

In ODE system (9) C_b , C_l , C_h , C_{is} and C_{br} are concentrations of the nanoagent in the blood, the liver, the heart, intercellular spaces of the brain and brain cells, respectively. Concentrations C are the variable values in differential equations of system (9). As per the constants K_e , K_l , K_h , K_{br} , these are the variables – associated parameters, i.e. the process rate coefficients which stands for drug pharmacokinetics as relates to either organ or intercellular space (K_{is}) distribution/accumulation.

The 'intercellular spaces' compartment was added into consideration to emphasize the striking difference in permeability of the blood brain barrier for ischemic lesions compared with non-affected brain regions. The K_{is} constant is adjusted with regard to the size of ischemic lesion: the bigger the inflammation focus, the higher its value. The “–” sign with the constant identifier indicates the reverse process, i.e. the removal of a nanoagent from an organ or tissue. The K_e constant reflects the nanoagent elimination. The rest of the constants reflect the rates of transition of nanoagent molecules between the compartments. It is easy to see that summation across the system leaves us with the term $K_e C_b$ only,

i.e. the nanoagent is completely eliminated from the body. For simplicity, the removal of the nanoagent through the liver is also included in K_e , but the metabolism takes time, which is reflected by the constants corresponding to the liver.

$$\begin{aligned}\frac{dC_b}{dt} &= -K_e C_b - K_{l+} C_b - K_{h+} C_b - K_{is+} C_b + K_{l-} C_l + K_{h-} C_h + K_{is-} C_{is} \\ \frac{dC_l}{dt} &= K_{l+} C_b - K_{l-} C_l \\ \frac{dC_h}{dt} &= K_{h+} C_b - K_{h-} C_h \\ \frac{dC_{is}}{dt} &= K_{is+} C_b - K_{br+} C_{is} - K_{is-} C_{is} + K_{br-} C_{is} \\ \frac{dC_{br}}{dt} &= K_{br+} C_{is} - K_{br-} C_{br}\end{aligned}\quad (9)$$

Knowing the half-life $T_{1/2}$, we can estimate the elimination constant K_e as

$$\ln 2 / T_{1/2}.$$

We modeled a single intravenous injection of the substance at a 0.2 mg/ μ g dose. Although the uniform distribution of a pharmacophore from the injection site throughout the body is known to take time, we excluded the 'diffusion' factor from the model to simplify calculations, that is, assumed the nanoagent concentration uniformity immediately after administration.

The *in silico* modeling curves in comparison with *in vivo* experimental data are shown in Fig. 8.

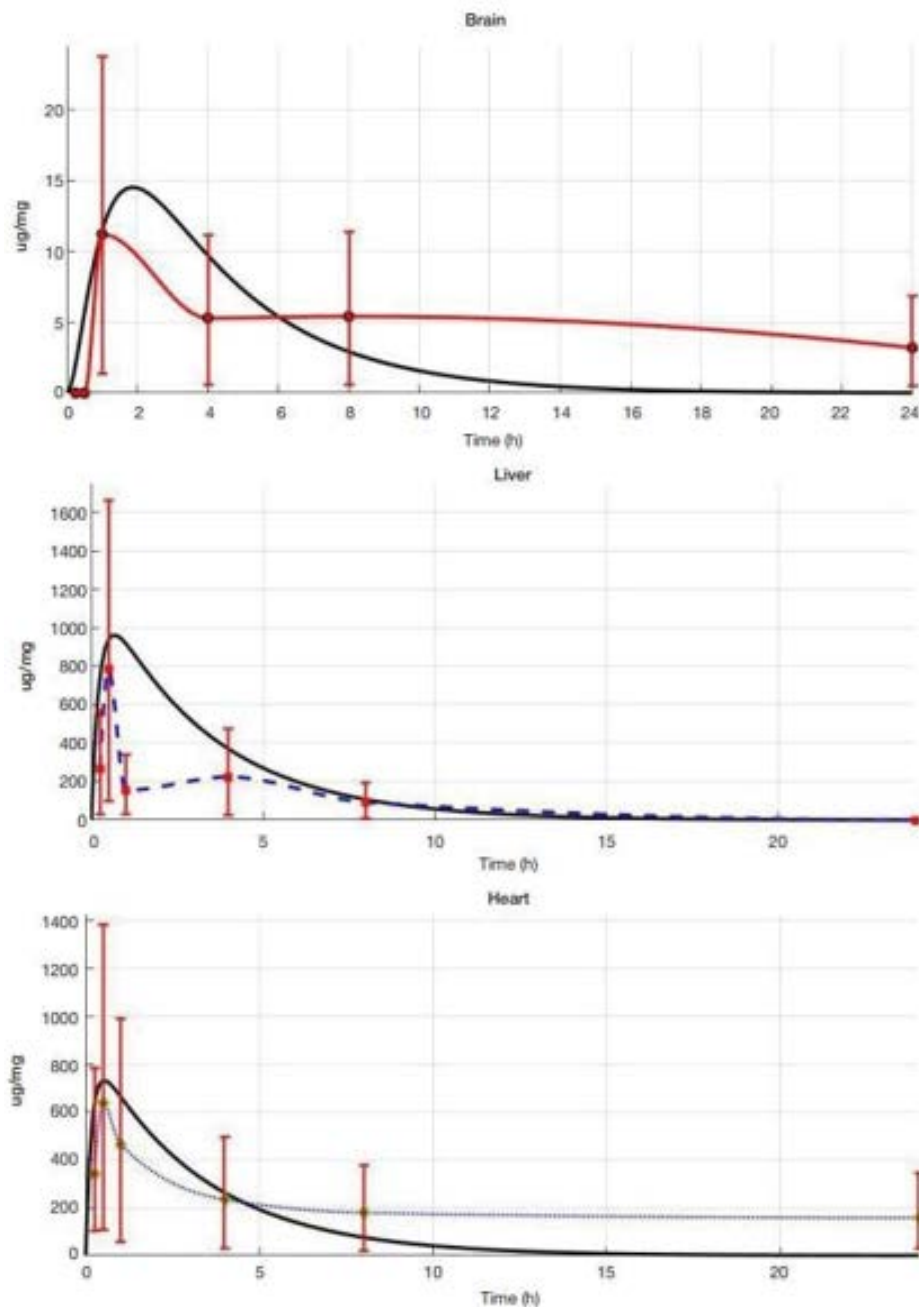


Figure 8: Pharmacokinetic curves built using the model (shown in black) compared with experimental data for the brain, the liver and the heart ($K_{hm} = 0.50$; $K_{lp} = 2$; $K_{hp} = 0.50$; $K_{lm} = 6$; $K_{hm} = 0.50$; $K_e = 0.077$; $K_{bp} = 0.70$; $K_{bm} = 0.70$; $K_{ism} = 0.10$; $K_{isp} = 0.10$)

The pharmacodynamics of the studied pharmacophore was simulated *in silico* over 24 h known to be the critical period of ischemic stroke development. With an increase in K_{h+} , the peak pharmacophore concentration in the myocardium shifts to the left and increases. According to published evidence [2], pharmacophore concentration rapidly peaks in the liver (within one hour) and declines rapidly, i.e. the liver clearance constant exceeds the absorption constant; at that, K_{h+} is smaller than K_{h-} . Upon a decrease in the clearance constant K_{h-} , the peak concentration of pharmacophore increases sharply. The corresponding constants describing pharmacodynamics for the brain require additional data for proper validation; nevertheless, Fig. 8 shows that pharmacophore accumulation in the brain is lower compared with the liver and the myocardium, which is consistent with both the literature [2], and our own *in vivo* experiments. Fig. 8 shows the calculated and experimental pharmacokinetic curves for PMC16 in the brain, the liver and the heart. The calculated curves (shown in black) have a classical shape and numerically fit into the confidence intervals of the experimental data collected *in vivo* for rat model, which proves the consistency between the mathematical model and the natural experiment.

Thus, we demonstrate experimentally that PMC16 crosses the blood-brain

barrier to be internalized by the post-ischemic brain cells, delivering 25Mg^{2+} ions that stimulate ATP hypersynthesis and thereby exert strong neuroprotective effects. At the same time, quantitative content of the studied pharmacophore in the brain, the heart and the liver differs. Our *in silico* model retrieves the same results, which confirms its prognostic potential and prospects in optimization of preclinical studies algorithms for porphyrin-fullerene nanocationites as promising neuroprotectants.

The distribution of PMC16 NPs in brain regions with regard to ischemic injury is given in Table 2.

Discussion

The paper [21] features the data from an *in vitro* and *in vivo* study experimentally modelling the syndrome of medication-induced hypoxia in myocardium and presents a broad spectrum of research into PMC16, including an experimental investigation of the PMC16 and its metabolites' pharmacodynamic and pharmacokinetic for various organs. In [21], reader can find data on the tissue-specific accumulation of PMC16 in rats after a single injection. Experiments register selective accumulation and protracted retention of non-metabolized molecules of the preparation exactly where the hypoxia was modelled in the aforementioned paper – in the myocardium cells. Similar dynamics was found under the conditions of the multiple injections course of ultra-low doses of PMC16, as evidenced by the data in [21]. At the same time, total absence of long-time capture of PMC16 was

observed in dealing with other tissues (liver, lungs, kidneys, skeleton muscles) [21]. The *In Silico* mathematical model presented in this paper yields completely adequate results on the qualitative level. This model adequately reflects the essence of the process discovered and helps to understand it mathematically.

Despite the good performance of the model presented in this article in the first approximation, one cannot but agree that it also has objective drawbacks, although the predictive and descriptive capabilities demonstrated by *In Silico* pharmacokinetics of targeted delivery of fullerene-porphyrin nanoparticles that release 25Mg^{2+} are described in this work, in a characteristic sense, are quite high. The model, built on the one-compartment principle, is, of course, adequate only for two of the parenteral modes of drug administration: intravenous and intra-arterial. It cannot numerically (and perhaps even characteristically) describe other methods, since it does not include the drug-specific features of other modes of administration.

Data of full-scale *in vitro* and / or *in vivo* experiments will be required at a certain stage to adjust the *In Silico* model to actual study objects. Normally this is performed through dynamic characteristics, which supplement the system of equations. These functions connect the values of the internal theoretical parameters 's', 'D', and 'e' to the actual objects. After that we can speak about the correlation of the numerical values of parameters to the actual objects and simulation studies, as well as on the complex combination of calculational and full-scale experiments to optimize pre-clinical studies.

Due to the fact that *In Silico* is built in a global (point) model, it also does not take into account the spatial factors of the spread of processes and substances. For these reasons, it is unsuitable for spatial modeling of hypoxia processes and diseases arising from this. But being a pharmacokinetic model, it is not required to solve such problems. For the same reason, its capabilities are severely limited for solving pharmacodynamic problems.

Undoubtedly, with the accumulation of experimental data, *In Silico* capabilities will improve. First of all, this concerns an increase in the compartmentalization of the model to take into account both additional methods of drug administration and the ways of its elimination. It is also of interest to supplement the capabilities of the model with pharmacodynamic and others modules, primarily due to the ability to describe the features of more subtle and complex intracellular Mg-dependent processes in relation to the therapeutic features of nanopreparations of the PMC16 line and taking into account the pathophysiology of ischemic stroke as we described in [32].

The main reason for the hindering development of the model is the lack of experimental data obtained *in vitro* and

in vivo, as well as the poorly studied at the biomedical level of a large number of processes and phenomena occurring in the body.

The development of *In Silico* is a related, but a separate fundamental task, the value of which is to identify the methods of mathematical description of very complex processes occurring in the body and to further implement *In Silico* models to solve applied tasks.

To verify our *In Silico* platform, the experimental estimation of PMC16 nanoparticles in the rat brain cytosol fraction has been proposed.

The pharmacokinetics of porphyrin-fullerene nanoagents for preclinical research optimization is solvable *in silico* on a computational experiment basis [32]. However, for comprehensive optimization of research algorithms, pharmacokinetics (PK) (i.e. computational output for the pharmacophore delivery to a particular organ, as has been done by us for PMC16 in this study) should be complemented by pharmacodynamics (PD) (i.e. a corresponding output for the development of therapeutic effect towards the studied pathology, e.g. ischemic stroke). We therefore consider building a complex PK/PD model as the ultimate prospective goal of our further research *in silico*.

Meanwhile, such studies are complicated not only by the scarcity of comprehensible mathematical models of ischemic stroke suitable for this purpose, but also by the lack of pharmacokinetic models for innovative pharmacophores, which may show distinct drug-specific pharmacokinetic patterns, especially under conditions of targeted delivery. The rapidly expanding field of nanopharmacology offers quite a number of such agents with excellent neuroprotective properties, albeit with pharmacokinetic patterns distinct from those of conventional pharmaceuticals [47].

These considerations are immediately applicable to the domestically produced PMC16, range regarded extraordinary promising in terms of ischemic stroke therapy. The invention of these pharmacophores was based on the fundamental discovery of the magnetic isotope effect exerted by $^{25}\text{Mg}^{2+}$. The magnetic isotope hyperactivates the magnesium-dependent ATP syntheses in a cell; moreover, such energy metabolism hyperactivation requires a tiny amount of these ions and can proceed even in the absence of oxygen, under conditions of profound tissue hypoxia [2]. These properties are exemplified by PMC-16 — a pharmaceutical nanoagent comprising a porphyrin-containing fullerene 'sphere' C60 (porfyllerene-MC16) [1,2].

The key issues in experimental validation of such *in silico* paradigm as ours include crossing of the blood-brain barrier by PMC16 and its capture (internalization) by brain cells. The task was accomplished (Fig. 8; Tables 1 and 2) to find both conditions fulfilled. Noteworthy, brain regions affected by the stroke were accessible to PMC16 as well (Table 2).

Thus, the relatively low 'mass quantity level' of NP capture by rat brain cells (Table 1) may have no correlation with the expected pharmacological effect of the agent, as the latter invariably involves the excessive ATP synthesis as a direct consequence of the $^{25}\text{Mg}^{2+}$ magnetic isotope effect phenomenon. At the same time, internalization of pharmacophore by target cells is definitely a priority in the advanced drug development.

A plain single-step ultracentrifugation (105,000–150,000 g) of mammalian tissue homogenates, usually pretreated with Triton X-100, ensures separation of cytosol from organelles, ribosomes, ribosomal subunits and membranous debris. The S125 fraction, a totality of soluble cytosolic compounds, is an excellent substrate to be used in pharmacophore internalization studies [48,49,50].

Although the obtained results are valuable as such, it should be noted that resolution and sensitivity of our CZE procedure are high enough to enable determination of the low-rate capture of PMC16-RX by rat brain, reaching estimated 4.0–8.0 ng per 1.0 mg of S125 total protein. Such content of NP, recorded 12 h after single intravenous injection of the drug, is distinctly above the background set by calibration (Table 1), which clearly indicates the penetration of the studied xenobiotic through the blood-brain barrier (Tables 1 and 2).

Materials and Methods

In Silico platform

To study the behavior of our model in the parameter space, we apply the theory of nonlinear dynamical systems and use a method known as "parametric analysis". In synergetics, it is more often called "bifurcation analysis". This method is effective for studying complex nonlinear processes in nonequilibrium systems of various types: physical, chemical, social, biological, etc. according to their mathematical models.

Here 's', 'D', and e parameters were not calculated but given within the stated ranges, which were used to calculate the variables in question (C_a and C_b – concentration of PMC16 nanoparticles in the blood flow and the intercellular space, respectively). Thus, the behavior of the model with different combinations of parameters was investigated.

The system of ordinary differential equations (8) was obtained by an analytical method based on the published data of biomedical studies of fullerene-porphyrin nanoparticles releasing $^{25}\text{Mg}^{2+}$ for the treatment of local hypoxia in the field of medical nanopharmacology and was simulated in MATLAB language in MATLAB / SIMULINK environment version 2021b. To solve the system of differential equations, the Runge-Kutta method of medium order was applied using the ode45 solver. A software programing code is under protection by the Russian Federation Patent law [51].

The data presented in $T_{1/2} = 9,0$ часов, $T_{max} = 25$ hours, $C_0 = 62$ µg/ml. For the parameters, arbitrary values were varied.

An updated five-compartment computational model was designed in a course of developments on the previous two-compartment model. This has been done once the experimental validation on PMC16 organs/tissues pharmacokinetics was performed. As seen from its graphical model presented in Figure 7, this model includes 5 differential equations suitable to describe the changes of PMC16 contents in those body compartments where this drug has been experimentally detected: blood, brain, heart, liver. These equations were obtained in a routine analytical way. For this model processing, the MATLAB/SIMULINK–2021B software version was employed. To solve a system of these differential equations, a Ronge-Kutt's conventional method was applied. A programing code was formalized in MATLAB language, this code now is under a legal protection provided by a registered Russian Federation Patent [52].

Due to the reasons we have given above it makes no sense to present some parameters in a separate table. The charts given in the article contain the required characteristic curves and are a much better representation of the meaning and the results of our research. The logics of Figure 7 is to present the original code of the software to satisfy the requirement of the editorial.

One of the most intriguing, truly attention catching, mark of this work relates to a specifically autonomous matter of the computational approach we proposed. Thus, *In Silico* platform is not about either to describe or treat the experimental data derived from the extensive and costly full-scale preclinical (clinical) trail. Instead, this entirely about how to predict, i.e. how to reveal pre empirico a highly probable patterns of pharmacokinetic processes based on available information regarding the known nanoparticle properties, disease model morphophysiological signs, tissue hypohia molecular and cellular pathogenesis mechanisms, etc.

Once succeeded, this approach is capable to provide with a reliable “navigator” information for further use in optimized design of preclinical research multidisciplinary protocols. A mere need for getting such a specific *In Silico* paradigm was, in fact, shown and clearly expressed in several studies [33-39] including the ones devoted to fullerene containing nanoparticles in the mammalian tissue hypoxia and brain research [40]. Likewise, some current developments in molecular kinetics computational models operates with both Gompertzian and non-Markov's population dynamics equasion systems [41], which is a rather promising tool that has been brought to the *In Silico* focused nanopharmacology community.

Experimental verification

Nanoparticles

Water soluble samples of PMC16-RX were kindly provided by a courtesy of Dr. N. Amirshahi, Amir Kabir University of Technology, Tehran, Iran.

Animals

Wistar Albino Glaxo male rats, 180 – 220 g, were kept under a standard vitaminized diet, starving for 24 hrs before experiment. Three animals per each experimental point, 5-6 repetitions for every measurement were carried out.

NP Administration

1.0 mg/kg and / or 20.0 mg/kg of NP was administered to rats in a single i.v. injection. Solvent: 15 mM Tris-HCL (pH 7.80). Animals were decapitated 12 hrs after injection, brain tissue samples were removed and homogenized in 5 – 7 vols of 20 mM Tris-HCL (pH 8.0) / 10 mM MgCl₂ / 1.5 mM NaCl / 2.0 mM EDTA / 25 mM sucrose / 2.0% Triton X-100 (v/v). Potter glass-teflone homogenizer, 1,800 r.p.m (+4 °C), has been employed.

Brain homogenate treatment

To isolate the cytosol fraction (S125), the carefully washed homogenates were subjected to ultracentrifugation at 125,000 g, 4 hrs, +4 °C, Spinco L5-65B Ultracentrifuge (Beckman, USA), rotor SW 27.1. Superatants (S125) were carefully collected, protein measurements were performed by a routine Bradford colorimetric method.

S125 samples were mixed with 10 vols of ice-cold acetone followed by an overnight incubation at +4 °C. The resulted pellets were precipitated at 20,000 r.p.m., 20 min, +4 °C and removed. Supernatants were collected for further use in UV-VIS spectrophotometry and CZE studies.

To elucidate the target product extractability degree, the acetone precipitated dry pellets were dissolved in 15 mM ammonium phosphate (pH 8.80) / 0.1% SDS / 2.5 mM EDTA / 1.0% 2-mercaptoethanol (20:1, v/w) with a consequent sonication treatment at 60 KHz, 40 °C, 60 min, followed by the below specified Capillary Zone Electrophoresis (CZE) analysis.

Ischemic stroke model

The filament insertion based modeling of ischemic stroke in rats was performed, using the middle cerebral artery occlusion as described in [46].

CZE Procedure

Acetone-soluble S125 extracts were concentrated in a rotor evaporizer to the final volume of 0.2 mL followed by addition of 30 mM ammonium-phosphate (pH 8.80), 25:1 (v/v).

10 μ L of a sample was inserted into the P/ACE MDQ Plus CZE Analytical System (ALGIMED, Belarus) coupled to the UV-VIS 770 KS detector, 440 nm monochromatic filter (Prince Technologies, Netherlands) with a following 10 min run at +6 °C: Quartz (50 μ diameter/ 7.5 cm effective length) capillaries packed with the UV-transparent silica saturated by SJX40 electrolyte – pH 8.80 (SCIEX BV, Netherlands), 115V / 60 Hz / 300 W per cap. Data acquisition unit: DAX DATE 220 LK (SCIEX BV, Netherlands). The corresponding calibration chart is stated in Table 1.

Table 1: The internal standard contents as correlated to absorbance of cze – revealed target compound (PMC16-RX, $R_t=7.0$ min)*

PMC16-RX, ng / mg S125 protein	A_{440} / mL (M \pm SEM)
1.0	0.09 \pm 0.02
5.0	0.33 \pm 0.08
10.0	0.61 \pm 0.09
25.0	1.84 \pm 0.08
50.0	3.87 \pm 0.11
100.0	5.32 \pm 0.50
200.0	8.55 \pm 0.72
1000.0	12.89 \pm 0.96

Table 2: BBB Permeability For Pmc16-Rx And The Drug Intratization In Brain Cells

Drug cytosol content, ng/mg S125 protein (M \pm SEM, n=6)		
INTACT BRAIN	PENUMBRA	STRIKE AREA
7.83 \pm 0.66	8.85 \pm 0.74	4.11 \pm 0.28

*Note: 20 mg PMC16-RX per 1.0 kg rat body weight, i.v., 12 hrs after a single injection, (see *Methods*).

Optimization of basic model

The article presents the basic author's model. In [56], we have taken steps to optimize the basic model described here in order to improve its flexibility, variability, and accuracy, and to adjust it to maximize compliance with experimental data and improve its predictive potential. While maintaining the general principles of building the initial model, several improved versions of the initial model are proposed. One of them has a model that takes into account the volume of cameras, the other has a built-in population dynamics algorithm known as the algorithm of interacting countries, which selected the values so that it optimized the points in the middle of the time interval. Two more variants contained duplicate chambers in order to more realistically account for the accumulation of nanopharmacophore in the intercellular space and organs that are not described by the basic model. In these variants, each camera receives a duplicate, with which it

is connected by incoming and outgoing flow. Then term (10) is added to each equation on the right side, where the values with the p index are the parameters of the main camera, and with the d index, the backup camera.

$$-k_{d+}C_pV_p + k_{d-}C_dV_d, \quad (10)$$

Two options were considered, when the experimental data are approximated by values from the main cameras and from their backups. The use of backup cameras can significantly improve the quality of prediction of the pharmacokinetic model in the case when the pharmacokinetic curves tend to a constant non-zero value, that is, there is an accumulation of substances in the tissues. At the same time, it is the main cameras that correspond to the organs. The stand-in chambers mimic the tissues surrounding the organ, where the drug or nanoparticles can stay for a long time, maintaining an almost constant level of the drug in the main chamber of the organ for a long time. Thus, 15 additional parameters were added to the basic model, representing volumes and speed constants in the backup cameras. It was possible to improve the approximation of peak values by varying the weight coefficients of the data. As a result of the optimizations carried out, the flexibility of model configuration and its variability have been improved. In addition, the obtained model variants more accurately approximated the peak and final values of the release curves.

Conclusions

As seen from some recent studies, mathematical and, more specifically, *computational* outlook is no doubt required for a better quality of molecular and cellular pathogenesis schemes. Thus, a simple experimental validation of the *In Silico* – derived statements on some ante *experimentum* designed biochemical scenaria of autoimmune [55], oncogenic [53, 55] and neurodegenerative [54] pathologies has already allowed to avoid a complex, time/resources consuming, lab testing programs with no harm to a final result such as an ethiopathogenesis concept and/or its essential upgrade.

In the present work:

1. Based on the analysis of literature data on the known properties of the promising antihypoxic nanopreparation PMC16, which is a monoadduct nanoparticle of iron-containing porphyrin with the classic buckminsterfullerene – buckminsterfullerene (C_{60})-2-(butadiene-1-yl)-tetra-(o- γ -aminobutyl)-ferroporphyrin, releasing $^{25}Mg^{2+}$, the unique antihypoxic effect of which is based on the magnetic isotope effect of the only magnetic isotope $^{25}Mg^{2+}$ in the family of magnesium isotopes, we for the first time obtained an elegant system of second-order equations, which was the basis *In Silico* of drug-specific pharmacokinetics of targeted delivery of nanoparticles and selective PMC tissues subjected to hypoxia.
2. This mathematical model, despite its apparent simplicity, simultaneously describes several complex processes

occurring during the transport of a nanopreparation to the hypoxia focus, and reflects the main drug-specific features of the pharmacokinetics of targeted delivery and selective accumulation of PMC16 in organs and tissues subjected to oxygen starvation (hypoxia). The model does not contradict the main characteristic features of pharmacokinetic curves in one- or two-compartment interpretation, and can be effective for computational experiments and development of scenarios for PMC16 preclinical studies as applied to the treatment of ischemic stroke, myocardial infarction and a number of oncological diseases for which Mg-dependent processes are important.

3. A two-compartment model reflects the key points of hypothesis on the PMC16 targeted delivery mechanism as long as the hypoxia – damaged brain area is the case. The latter are known for their inflammation processes and, hence, for a sharp increase of the capillary endothelial pore sizes, which makes easier the intralization of medicinal nanoparticles.
4. An original advanced five-compartment model is just the “expanded version” of our basic two-compartment platform completed and validated with experimental (CZE) pharmacokinetic data. In both quality and quantitative aspects, this advanced model meets all expectations describing the drug concentration trends in organs studied. A clear correspondence of the model predictory potential to experimentally proven pharmacokinetic results makes it possible to conclude that our *In Silico* algorithms are suitable for applied use in a preclinical research protocol.
5. From a practical point of view, a novel *In Silico* systematic directory proposed might indicate a perspective for clear and essentially simplified plan making required to design an optimized protocol suitable for the $[^{25}\text{Mg}^{2+}]_4$ PMC16 – related preclinical research program. This suppose to get realized by taking into account an anti-hypoxia pharmacological potential of these medicinal nanoparticles in the brain ischemic disorders (stroke) studies.

Besides, to the best of our knowledge, this work is a first report ever to prove an efficiency of combination of the *In Silico* modeling pharmacokinetics – related studies with the CZE – engaging analytical validation and outlook.

Author Contributions

Dr. V.V. Fursov: mathematical modeling per se, data analysis, conclusions, design of the manuscript. Prof. Dr. D.A. Kuznetsov: biomedical aspects of the brain ischemia models, data collection and analysis, antihypoxic NP specificity and magnetic isotope effects to take into account, conclusions. PhD student Daria Zinchenko: program code.

Funding

Work was supported by grant of Ministry of Science and

Higher Education of Russian Federation № 075-15-2020-792 (Unique identifier RF----190220X0031).

Acknowledgments

Prof. Dr. Eleonora M. Koltsova, Dr. Ivan I. Mitrichev, PhD student Roman S. Krashennnikov, Moscow, Russian Federation, are to be sincerely thanked for their kind assistance with preparation of a manuscript, consultations and for their encouraging comments on this work.

Conflicts of Interest

No conflicts of interests of any sort beyond.

References

1. Sarkar S, Rezayat S M, Buchachenko A L, et al. New water soluble porphyrin compounds. European Union Patent № 07009882.7/EP07009882 (2007).
2. Sarkar S, Rezayat S M, Buchachenko A L, et al. Use of a magnesium isotope for treating hypoxia and a medication comprising the same. European Union Patent № 07009881.9/EP07009881 (2007).
3. Buchachenko A L, Kuznetsov D A, Arkhangelsky S E, et al. Spin biochemistry: magnetic ^{24}Mg - ^{25}Mg - ^{26}Mg isotope effect in mitochondrial ADP phosphorylation. Cell Biochemistry and Biophysics 43 (2005): 243-252.
4. Buchachenko A L, Kuznetsov D A, Arkhangelsky S E, et al. Spin biochemistry: intramitochondrial nucleotide phosphorylation is a magnesium nuclear spin controlled process. Mitochondrion 5 (2005): 67-70.
5. Buchachenko A L, Kuznetsov D A, Orlova M A, et al. Magnetic isotope effect of magnesium in phosphoglycerate kinase phosphorylation. Proceedings of the National Academy of Sciences of the United States of America 102 (2005): 10793-10797.
6. Buchachenko A L, Kuznetsov D A, Breslavskaya N N, et al. Magnesium isotope effects in enzymatic phosphorylation. J. Phys. Chem., series B 112 (2008): 2107-2114.
7. Kano K. Molecular complexes of water-soluble porphyrins. J. Porph. Phthalocyanines 8 (2004): 148-155.
8. Hudson R, Mallroy C, Darnell S, et al. Porphyrin conjugates in photodynamic therapy. Brit. J. Cancer 93 (2006): 1442-1450.
9. Pawar R, Avramoff A, Domb A J. Nanoparticles for Crossing Biological Membranes. In: Biological and Pharmacological Nanomaterials (Kumar, C.S.S.R., Ed.) (2007): 349-393.
10. Bucyachenko A L, Tyutyunnik V M. New frontiers in gene chemistry. In: Prospective Areas of Research in Science and Technology (Tyutyunnik V.M., Ed.) (2021): 144-158.

11. Liu Y, Zeng S, Ji W, et al. Emerging theranostic nanomaterials and its complications. *Advanced Science*, 2102466, Wiley – VCH, GmbH: Heidelberg – Berlin (2021).
12. Pinheiro R G R, Coutinho A J, Pinheiro M, et al. Nanoparticles for targeted brain drug delivery: what do we know? *International Journal of Molecular Sciences* 22 (2021): 11654.
13. Sharoyko V V, Shemchuk O S, Meschcheriakov A A, et al. Biocompatibility, antioxidant activity and photoprotection properties of C60 fullerene adducts. *Nanomedicine: Nanotechnology and Medicine* (2021).
14. Andrievsky G, Klochkov V, Derevyanenko L. Is C60-fullerene molecule toxic? *Fullerenes, Nanotubes, Carbon Nanostructures* 13 (2005): 363-376.
15. Pantarotto D, Tagmatarchis N, Bianco A, et al. Synthesis and biological properties of fullerene-containing amino acids and peptides. *Minirev. Med. Chem* 4 (2004): 805-814.
16. Buchachenko A L. *Magneto-Biology and Medicine*. Nova Biomedical Publ.: New York (2015).
17. Naz S, Bashir F. Dual use research of concern. *Pakistan Journal of Medical Research* 58 (2019): 153-155.
18. J. J. Augsburg, C. M. L. Chow, V. Dyer, et al. Translating science into survival. In: *St. Jude's Children's Research Hospital Report* (Cajjar, A. & Pappo, A., Eds.); St. Jude's CRH Publ.: Memphis, TN — Cincinnati, OH: 6-55 (2016).
19. Bozic I and Nowak M A. Resisting resistance. *Ann. Rev. Cancer Biol* 1 (2017): 203-221.
20. Gusev E I, Skvorcova V I. *Ishemiya golovnogo mozga*. Medicina, Moscow (2001): 328
21. Amirshahi N, Alautdin R N, Sarcar S, et al. Porphyrin – fullerene nanoparticles in the hypoxic cardiopathies treatment. *Russian Nanotechnol* 3 (2008): 99-109.
22. Piotrovsky L B, Kiselyov O.I. *Fullerenes in Biology: On the Way towards Nanomedicine*. Rostok Publ.: St. Petersburg (2006).
23. Suarez M, Verdecia Y, Illescas B, et al. Synthesis and study of novel fulleropyrrolidines bearing biologically active 1,4-dihydropyridines. *Tetrahedron* 59 (2003): 9179-9186.
24. Tabata Y, Ikada Y. Biological functions of fullerenes. *Pure Appl. Chem* 71 (1999): 2047-2053.
25. Waugh T and Telashima H. *Mitochondria*. Research Triangle Publ.: Raleigh- Durham, NC (2004).
26. Gergely M and Lakatos I. *Molecular and Cellular Cardiology*. Alba Regia: Budapest-Szeged (1999).
27. Pawar R, Avramoff A, Domb A J. Nanoparticles for Crossing Biological Membranes. In: *Biological and Pharmacological Nanomaterials* (Kumar, C.S.S.R., Ed.) (2007): 349-393.
28. Mahatoo R. Biological membranes and barriers. In: *Biomaterials for Delivery and Targeting of Proteins and Nucleic Acids* (Telashima, I. & Waugh, J.A., Eds.) (2005): 241-260.
29. Baierl T, Siedel A. The in vitro effects of fullerene black on immunofunctions of macrophages. *Fullerene Sci. Technol* 4 (1996): 1073-1085.
30. Mellul M. Cosmetic make-up composition containing a fullerene or mixture of fullerenes. US Patent № 561202 (1997).
31. Leone J E, Narayanan P V. Catheter system having fullerenes and metod. US Patent № 6468244 (2002).
32. Fursov V V, Fursov I V, Bukhvostov A A, et al. In Silico Studies on Pharmacokinetics and Neuroprotective Potential of $^{25}\text{Mg}^{2+}$: Releasing Nanocationites – Background and Perspectives. In: *Pharmacogenetics*, (Khalil I.A., Ed.) (2021): 30-48.
33. Bray D. Limits of computational biology. *In Silico Biology* 12 (2015): 1-7.
34. Maynard A T, Roberts C D. Quantifying, vizualizing, and monitoring lead optimization. *J. Med. Chem* 59 (2016): 4189-4201.
35. Wooller S K, Benstead-Hume G, Chen X, et al. Bioinformatics in translational drug discovery. *Bioscience Reports* (2017).
36. Rajah G B, Ding Y. Experimental neuroprotection in ischemic stroke: a concise review. *Neurosurg. Focus* 42 (2017).
37. Fatima S, Quadri S N, Parveen S, et al. Nanomedical strategies as emerging therapeutic avenues to treat and manage cerebral ischemia. *CNS Neurol. Disord. Drug Targets* 20 (2021): 125-144.
38. Paul S, Candelario J E. Emerging neuroprotective strategies in the treatment of ischemic stroke: An overview of clinical and preclinical studies. *Experimental Neurology* (2021).
39. Skvortsov V S, Ivanova Y O, Voronina A I. The bioinformatic identification of proteins with varying levels of post-translational modifications in experimental ischemic stroke in mice. *Biomed. Chem* 67 (2021): 475-484,
40. Kazemazadeh H, Mozafari M. Fulleren-based delivery systems. *Drug Delivery Today* 24 (2019): 898-905.
41. Glielmo A, Husic B E, Rodriguez A, et al. Unsupervised

- learning methods for molecular simulation data. Chemical Reviews (2021).
42. Sener R N. Diffusion MRI: apparent diffusion coefficient (ADC) values in the normal brain and a classification of brain disorders based on ADC values. Comput Med Imaging Graph 25 (2001): 299-326.
 43. Haaga, John Robert and Daniel T. Boll. "CT and MRI of the whole body (2017).
 44. Helenius J, Soinne L, Perkiö J, et al. Diffusion-weighted MR imaging in normal human brains in various age groups. AJNR Am J Neuroradiol 23 (2002): 194-199.
 45. Annet L, Duprez T, Grandin C, et al. Apparent diffusion coefficient measurements within intracranial epidermoid cysts in six patients. Neuroradiology 44 (2002): 326-328.
 46. Gubsky I L, Namestnikova D D, Cherkashova E A, et al. MRI guiding of the middle cerebral artery occlusion in rats aimed to improve stroke modeling. Translational Stroke Research 9 (2018): 417-425.
 47. Amirshakhi N. I dr. Porfirin-fullerenovye nanochastitsy dlya lecheniya gipoksicheskikh kardiopatii. Rossiyskie nanotekhnologii 3 (2008): 125-135.
 48. Benjamin D J, Prasad V, Lythgoe M.P. FDA decisions on new oncological drugs. Lancet Oncology 23 (2022): 585-586.
 49. Das M. Biden's proposed investment in cancer research sparks concerns. Lancet Oncology 23 (2022): 576-580.
 50. Orlova M A, Osipova E Y, Roumiantsev S.A. Effect of 67Zn-nanoparticles in leukemic and normal lymphocytes. British Journal of Medicine and Medical Research 2 (2012): 21-30.
 51. Fursov V.V. PMC16: Pharmacokinetic stroke 2C-model. Russian Federation Patent, 2022664091/EQNNJQ (2022).
 52. Zinchenco D I, Fursov V V, Ananiev A.V. The Computational mode for pharmacokinetics of the porphyrin-fullerene nanopharmacofores in organs and tissues. Russian Federation Patent, 20222684064/KRWUJW (2023).
 53. Anders J S, Delbreux B S, Kolchin M M. Predictions and algorithms in computational medicine. In: Frontier in Medical Biology (2022): 128-143.
 54. Beitollary R M, Boushehri N, Ter-Kazarian M, et al. Mathematical modeling of cellular and molecular disequilibria in pathologically damaged biological systems. Amir Kabir University of technology Reports, Series C 48 (2021): 22-38.
 55. Di Marco M, Luchinat G, Tomassetti L, et al. Non – Markov population dynamics to check the most doubtful predictions in medicinal thresholds. Acta Academiae Pontifica, LXXIV (2020): 216-240.
 56. Krashennnikov R S, Mitrichev I I, Fursov V V. Using the pypharm library for pharmacokinetic modeling of porphyrin-fullerene nanoparticles. Modern high technologies 4 (2025): 30-42.



This article is an open access article distributed under the terms and conditions of the
Creative Commons Attribution (CC-BY) license 4.0